

UAV Swarm Deployment and Trajectory for 3D Area Coverage via Reinforcement Learning

Jia He^{1,2}, Ziyi Jia^{1,2*}, Chao Dong¹, Junyu Liu², Qihui Wu¹, and Jingxian Liu³

¹The Key Laboratory of Dynamic Cognitive System of Electromagnetic Spectrum Space, Ministry of Industry and Information Technology, Nanjing University of Aeronautics and Astronautics, Nanjing, Jiangsu, 210016

²State Key Laboratory of Integrated Services Networks (Xidian University), Xi'an, 710071

³Ericsson (China) Communications Company Ltd., Beijing, 100102

*Email: jiaziye@nuaa.edu.cn

arXiv:2309.11992v1 [eess.SP] 21 Sep 2023

Abstract—Unmanned aerial vehicles (UAVs) are recognized as promising technologies for area coverage due to the flexibility and adaptability. However, the ability of a single UAV is limited, and as for the large-scale three-dimensional (3D) scenario, UAV swarms can establish seamless wireless communication services. Hence, in this work, we consider a scenario of UAV swarm deployment and trajectory to satisfy 3D coverage considering the effects of obstacles. In detail, we propose a hierarchical swarm framework to efficiently serve the large-area users. Then, the problem is formulated to minimize the total trajectory loss of the UAV swarm. However, the problem is intractable due to the non-convex property, and we decompose it into smaller issues of users clustering, UAV swarm hovering points selection, and swarm trajectory determination. Moreover, we design a Q-learning based algorithm to accelerate the solution efficiency. Finally, we conduct extensive simulations to verify the proposed mechanisms, and the designed algorithm outperforms other referred methods.

Index Terms—UAV swarm, 3D area coverage, swarm trajectory planning, reinforcement learning.

I. INTRODUCTION

UNMANNED aerial vehicles (UAVs) are recognized as promising solutions to tackle area coverage problems (ACPs) due to the inherent mobility and flexibility. In addition, UAVs are widely used in various practical scenarios, such as wireless data collection, mapping, disaster rescue, reconnaissance and surveillance [1]–[4]. However, as for a single UAV, the limitations of payload, size, energy capacity, etc., impact its service ability [5]. Thus, a single UAV may not ensure sufficient and reliable wireless communication services for ground users (GUs) [6]. Fortunately, the UAV swarm, consisting of multiple small UAVs, can establish seamless wireless communication services for large-area GUs. However, the following challenges related to the UAV swarm still should be handled: 1) the efficient cooperation of UAVs to serve multiple GUs; 2) how to deploy the UAV swarm to achieve a tradeoff between coverage and energy efficiency; 3) the trajectory planning for the swarm considering the effects of

obstacles. Hence, it is essential to design a reasonable UAV swarm framework and efficient trajectory plan for large-scale 3D area coverage.

There exist a couple of recent works related to UAVs in ACPs scenarios. For instance, Zhao *et al.* in [7] study the 3D mobile sensing and trajectory optimization problem with a single UAV. In [8], Zeng *et al.* investigate energy-efficient UAV communication by deriving a paradigm related to UAV's energy consumption and trajectory planning. He *et al.* in [9] consider the 3D UAV deployment problem in uneven terrains for GUs' connectivity and coverage. Jia *et al.* in [10] present a matching game theory-based algorithm to deal with the offloading decisions from users to UAVs. Hou *et al.* in [11] propose a joint neural network to optimize both the transmission power and the user association in a multi-UAV communication system with moving users. In [12], the utilization of UAV swarms shows improved coverage performance for ACPs. However, as far as the authors' knowledge, the above works lack considering deployment and trajectory planning for UAV swarms, which is a significant issue.

Hence, in this work, we consider a large-scale 3D coverage scenario with non-uniformly distributed GUs. Then, we design a hierarchical UAV swarm framework consisted of a cluster head UAV (H-UAV) and tail UAVs (T-UAVs) to efficiently accomplish the coverage mission. In particular, we divide the large-scale 3D area into discrete space considering obstacles. Then, the ACP is formulated as an optimization problem to minimize the total trajectory loss of the UAV swarm. Due to the non-convex property, we further decompose it into smaller problems of GUs clustering, UAV swarm hovering points (HPs) selection and trajectory planning. Then, we design a K-means clustering based method to cluster GUs and select the optimal HPs as deployment positions to satisfy the coverage requirements. Then, we model the trajectory planning problem as a Markov decision process (MDP) to depict the complex environment. Then, a Q-learning based UAV swarm trajectory planning algorithm (QLUTP) is designed to handle the problem. Finally, we conduct extensive simulations to verify the effectiveness of the proposed methods.

This work was supported in part by the Natural Science Foundation of Jiangsu Province of China under Project BK20220883, and in part by the Natural Science Foundation on Frontier Leading Technology Basic Research Project of Jiangsu BK20222013.

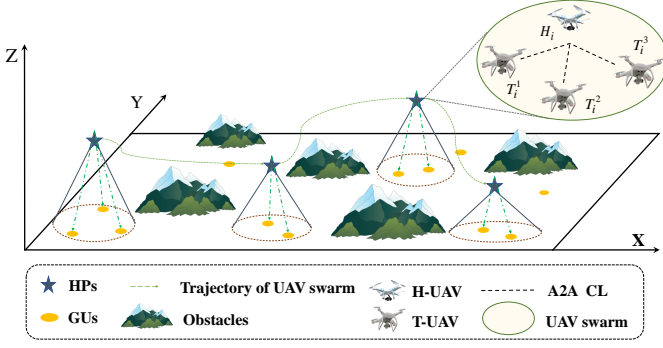


Fig. 1. UAV swarm enabled 3D area coverage scenario.

This paper is organized as follows. In Section II, we present the system model of large-scale 3D area coverage and provide the problem formulation. Section III proposes the algorithms of deployment and trajectory planning for the UAV swarm. Further, Section IV conducts simulations and analyzes the results to verify the proposed mechanisms. Finally, conclusions are drawn in Section V.

II. SYSTEM MODEL AND PROBLEM FORMULATION

A. 3D Area Coverage Scenario

As shown in Fig. 1, we consider a UAV swarm enabled coverage scenario, including a UAV swarm and a set of GUs. In general, it is assumed that all UAVs fly with a constant speed at the same altitude h within $[h_{\min}, h_{\max}]$. Further, GUs are non-uniformly distributed in the coverage area, denoted as $D = (u_1, u_2, \dots, u_M)$. During the flight, the UAV swarm needs to select N HPs, i.e., $\Omega = \{q_1, q_2, \dots, q_N\}$, to satisfy the coverage requirements.

In this work, we adopt the regular grid method to describe the large-scale 3D space, denoted as \mathcal{G} [13]. Specifically, \mathcal{G} is abstracted as an $L_x \times L_y \times L_z$ cuboid composed of small cubes with length of Δl . The center coordinates of the cube are presented as (x, y, z) . Further, the number of cubes is $N_x \times N_y \times N_z$, i.e.,

$$N_x = \left\lceil \frac{L_x}{\Delta l} \right\rceil, N_y = \left\lceil \frac{L_y}{\Delta l} \right\rceil, \text{ and } N_z = \left\lceil \frac{L_z}{\Delta l} \right\rceil, \quad (1)$$

in which the ceil function $\lceil f(x) \rceil$ returns the value of a number rounded upward to the nearest integer. The partition accuracy Δl is a hyper-parameter, and smaller Δl indicates that the accuracy of space \mathcal{G} increases. However, due to the searching and storage consumption, the computational complexity generally grows exponentially with slight decline of Δl . Therefore, it is essential to make comprehensive analysis according to the performance constraints of the UAV swarm and the practical scale of ACPs.

Moreover, it is necessary to consider the distribution of obstacles in the 3D space \mathcal{G} to avoid unnecessary collisions. In detail, the obstacle is described as $\{O|(x^o, y^o), Ob(x^o, y^o)\}$,

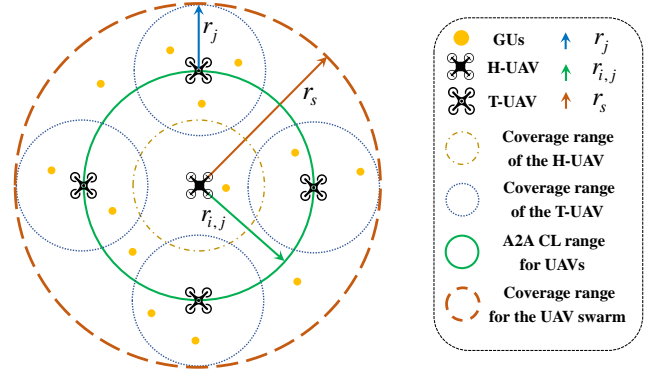


Fig. 2. An illustration of the coverage rate within a UAV swarm.

where (x^o, y^o) is the projection of a certain point on the horizontal plane, and $Ob(x^o, y^o)$ is the height of the corresponding obstacle point. Further, flag \mathcal{L}_{ob} represents the collision, i.e.,

$$\mathcal{L}_{ob} = \begin{cases} 0, & \mathcal{C} \notin O, \\ 1, & \mathcal{C} \in O, \end{cases} \quad (2)$$

where \mathcal{C} is the position of the UAV swarm. $\mathcal{L}_{ob} = 0$ means there exist no collisions between UAVs and obstacles. Otherwise, $\mathcal{L}_{ob} = 1$ represents there exist collisions.

Theoretically, the UAV swarm can fly above each GU for area coverage. However, this deployment policy results in additional energy consumption due to repeated coverage. Also, there are some isolated GUs which cannot be effectively covered. Therefore, a tradeoff between the coverage and energy performance should be considered. We define the GUs coverage rate Υ as an index to evaluate the coverage performance of the UAV swarm. In detail,

$$\Upsilon = \frac{1}{M} \sum_{n=1}^N A_n, \quad (3)$$

in which A_n is the number of covered GUs at n th HP, i.e., $q_n \in \Omega$. M represents the total number of GUs located in the area. In Fig. 2, an illustration of the coverage rate within a UAV swarm is provided. Since the coverage radius r_s of the UAV swarm is related with Υ , it is calculated as:

$$r_s = r_j + r_{i,j}, \quad (4)$$

where $r_{i,j}$ represents the communication radius between H-UAV and T-UAV, and r_j is the coverage radius of single T-UAV.

B. UAV Swarm Model

We propose a hierarchical UAV swarm framework composed of multiple small low-cost UAVs. All UAVs can be divided into two categories according to different roles in the swarm. H-UAV, acting as the leader of the swarm, can establish wireless communication links with other UAVs or ground base station for data transmission. T-UAVs, acting as followers, perform

the coverage mission with the leadership of H-UAV. Thus, the UAV swarm is defined as $\{H_i, T_{i,1}, \dots, T_{i,j}, \dots, T_{i,K}\}$, in which H_i and $T_{i,j}$ represent H-UAV and j th T-UAV of swarm i , respectively. In the swarm, we adopt the star topology, i.e., the H-UAV serves as the communication center and directly communicates with all T-UAVs. Besides, it is assumed that T-UAVs can only communicate with the H-UAV within the same swarm.

C. Communication Model

1) *A2A Communication Model*: We adopt the typical air-to-air (A2A) communication link (CL) model to characterize the communication model between the H-UAV and T-UAV [14]. Firstly, the position of H-UAV H_i and T-UAV $T_{i,j}$ are denoted by \mathcal{I}_i and $\mathcal{I}_{i,j}$, respectively. Then, the received power of H-UAV from T-UAVs is:

$$P_{r,H}(\mathcal{I}_i, \mathcal{I}_{i,j}) = P_{C,T} + G_t + G_r - P_l(\mathcal{I}_i, \mathcal{I}_{i,j}), \quad (5)$$

where G_t and G_r are the constant antenna gains of T-UAV and H-UAV, respectively. $P_{C,T}$ is the constant transmission power for UAVs. $P_l(\mathcal{I}_i, \mathcal{I}_{i,j})$ is the large-scale fading coefficient, defined as:

$$P_l(\mathcal{I}_i, \mathcal{I}_{i,j}) = 10a \log_{10} \left(\frac{4\pi \|\mathcal{I}_i - \mathcal{I}_{i,j}\|_2 f_c}{v_c} \right), \quad (6)$$

where $a > 0$ is the trajectory loss exponent, v_c is the speed of light, and f_c is the electromagnetic wave frequency [15].

In addition, the H-UAV and T-UAV establish a CL if the received power satisfies:

$$P_{r,H}(\mathcal{I}_i, \mathcal{I}_{i,j}) \geq P_0, \quad (7)$$

where P_0 is set as the threshold power. Based on (7), the Euclidean distance $\|\mathcal{I}_i - \mathcal{I}_{i,j}\|_2$ between H_i and $T_{i,j}$ satisfies:

$$\|\mathcal{I}_i - \mathcal{I}_{i,j}\|_2 \leq \frac{v_c}{4\pi f_c} \exp \left\{ \frac{\ln(10)}{10a} (P_{C,T} + G_t + G_r - P_0) \right\}. \quad (8)$$

Note that the horizontal distance between H_i and $T_{i,j}$ is equal to the Euclidean distance, $r_{i,j} = \|\mathcal{I}_i - \mathcal{I}_{i,j}\|_2$.

2) *A2G Link Model*: As shown in Fig. 1, T-UAVs provide effective signal coverage for corresponding GUs in the target area. In the air-to-ground (A2G) communication model, the channel gain of the line-of-sight link between T-UAVs and GUs is:

$$h_{j,m}^{A2G} = \frac{\beta_0}{d_{j,m}^2}, \quad (9)$$

where β_0 is the channel gain at the reference distance of each meter, and $d_{j,m}$ represents the Euclidean distance between $T_{i,j}$ and u_m [16]. Let $P_{m,j}$ represent the transmitting power of GU u_m , and the transmission rate is expressed as:

$$R_{j,m} = B \log_2 \left(1 + \frac{P_{m,j} h_{j,m}^{A2G}}{B\eta} \right), \quad (10)$$

where B and η are channel bandwidth and noise power density, respectively. The transmission rate $R_{j,m}$ should be not less than the minimum achievable rate threshold R_{Th} , i.e.,

$$R_{j,m} \geq R_{Th}, \quad (11)$$

which guarantees that the T-UAV can establish a stable CL with the GU. According to (9) and (10), we obtain the maximum coverage range $d_{j,m}$ of T-UAV as:

$$d_{j,m} = \sqrt{P_{m,j} \beta_0 / (2^{R_{j,m}/B} - 1)}, \quad (12)$$

where the transmission rate $R_{j,m}$ is equal to threshold R_{Th} . Then, the coverage radius of a single T-UAV is calculated as:

$$r_j = \sqrt{d_{j,m}^2 - h^2}, \quad (13)$$

where h is the flight altitude of the UAV swarm.

D. Problem Formulation

Since ACP aims to save energy via appropriate deployment of the UAV swarm, the objective is to minimize the flight trajectory loss of the UAV swarm. Thus, the optimization problem is detailed as:

$$\mathbf{P0} : \min_{\rho} (\Delta l \sum_{\rho \in \mathcal{P}} E d_n^{n+1})_{\Omega(q_1 \rightarrow q_N, \mathcal{Y})}, \quad (14a)$$

$$\text{s.t. C1: } \rho \in \mathcal{P}, \quad (14b)$$

$$\text{C2: } \mathcal{L}_{ob} = 0, \quad (14c)$$

$$\text{C3 - C4: } (7), (11), \quad (14d)$$

$$\text{C5: } \mathcal{Y} \geq \mathcal{Y}_{Th}, \quad (14e)$$

where variable ρ is a swarm trajectory path, Δl is trajectory loss for each step, and $E d_n^{n+1}$ is the number of path steps from q_n to q_{n+1} . All the HPs satisfying the coverage rate \mathcal{Y} are denoted as $\Omega(q_1 \rightarrow q_N, \mathcal{Y})$. Further, in constraint C1, the UAV swarm should fly within the tolerable space, i.e., $\rho \in \mathcal{P}$. Constraint C2 addresses the distribution of obstacles, in which flag $\mathcal{L}_{ob} = 0$ means there exist no collisions. As illustrated in C3, the received power $P_{r,H}$ should be not less than the limited threshold P_0 . In constraint C4, transmission rate $R_{j,m}$ should not less than threshold R_{Th} . Constraint C5 guarantees that the selected HPs satisfy the limitation of coverage rate \mathcal{Y} . Thus, \mathcal{Y}_{Th} is set to ensure the basic coverage performance. Due to the objective is to minimize the flight trajectory loss of the UAV swarm, both the deployment positions selection and trajectory planning are non-convex. As for the problem complexity, the solution space grows exponentially with the problem scale due to the non-convex property of $\mathbf{P0}$, which is intractable via a traditional optimization approach.

III. DEPLOYMENT AND TRAJECTORY PLANNING FOR THE UAV SWARM

To efficiently deal with $\mathbf{P0}$, we decompose it into smaller problems of GUs clustering, HPs selection for UAV swarm and trajectory planning. Firstly, in Section III-A, a K-means based

Algorithm 1 GUs Clustering and Hovering Points Selection

- 1: **Initialize** the deployment of GUs $\{u_1, u_2, \dots, u_M\}$, the coverage radius r_s and the number of clusters N .
 - 2: Create N points randomly as the starting centroid.
 - 3: **for** $episode = 1$ to MAX_{eps} **do**
 - 4: Reset the starting clusters $\{C_1, C_2, \dots, C_N\}$ as \emptyset .
 - 5: **for** GUs $i \in [1, M]$ **do**
 - 6: Calculate the Euclidean distance between the centroid and each data point.
 - 7: Assign the data point to the nearest cluster.
 - 8: **end for**
 - 9: **for** cluster $n \in [1, N]$ **do**
 - 10: Reset the centroid of each cluster.
 - 11: **end for**
 - 12: **end for**
 - 13: Count the number of data points within the coverage radius r_s for each cluster.
 - 14: Calculate the coverage rate Υ according to (3).
 - 15: **Return** the positions of updated clusters $\{C_1, C_2, \dots, C_N\}$ and the coverage rate Υ .
-

method is designed to cluster GUs, and select multiple HPs as deployment positions for the UAV swarm. Then, the ACP is modeled as an MDP in Section III-B. Further, a Q-learning based UAV swarm trajectory planning (QLUTP) is designed in Section III-C to minimize the flight trajectory loss.

A. GUs Clustering and HPs Selection

We adopt the K-means clustering based method to select optimal deployment positions of HPs. The variable $\Omega(q_1 \rightarrow q_N, \Upsilon)$ and N depend on the dispersion degree of GUs and the scale of the coverage area. The details of GUs clustering and HPs selection approach are presented in Algorithm 1. Firstly, we initialize the deployment of GUs $\{u_1, u_2, \dots, u_M\}$, the coverage radius r_s and number of clusters N . From step 3 to 12, GUs are clustered according to the distance and obtain the updated clusters. Further, we analyze the coverage range conditions of GUs in each cluster, as shown in step 13. Finally, we obtain the deployment positions of HPs satisfying coverage constraints, as illustrated from step 14 to 15.

B. MDP for Trajectory Planning

Reinforcement learning (RL) studies the sequential decision-making process, in which the agent acts as the subject body and interacts with the objective environment. Correspondingly, the UAV swarm is abstracted as an agent in the environment \mathcal{G} with obstacles. Thus, the optimization problem **P0** is reformulated in the form of MDP. An MDP problem is defined by a tuple $\{S, A, P, R, \gamma\}$, where S is the state space. A is the action space. $\{P : S \times A \rightarrow \Delta(S)\}$ is the state transition probability function from state $s \in S$ to another state $s' \in S$ with action $a \in A$. $\{R : S \times A \rightarrow \mathcal{R}\}$ is the immediate reward function of the agent, and $\gamma \in [0, 1]$ is a discounted factor. In addition, π

Algorithm 2 QLUTP for Trajectory Planning

Input: $N, \alpha, \gamma, \varepsilon$ and Δl .

Output: Optimal policy π^* .

- 1: **Initialize** action value table \mathcal{Q} arbitrarily according to $Q(s, a), \forall s \in S, a \in A(s)$.
 - 2: **Repeat** (for each episode)
 - 3: Initialize state space S .
 - 4: Choose action $a \in A$ under $s \in S$ with the proposed policy $\varepsilon(\text{ep})$ -greedy derived from table \mathcal{Q} .
 - 5: Take action A , observe R and S' .
 - 6: Update table \mathcal{Q} according to the formulation $Q(S, A) \leftarrow Q(S, A) + \alpha [R + \gamma \max_a Q(S', A) - Q(S, A)]$.
 - 7: $S \leftarrow S'$.
 - 8: **Until** S is terminal.
-

represents the policy, and $Q_\pi(s, a)$ represents the action value function.

1) *State space:* The state space S indicates the environment of the agent. In order to make the agent aware of the environment state, we introduce the positions of HPs $\Omega(q_1 \rightarrow q_N, \Upsilon)$ and obstacles $\{O|(x^o, y^o), Ob(x^o, y^o)\}$.

2) *Action space:* The action space provides six actions for the agent, i.e., $A = \{a_f, a_b, a_r, a_l, a_u, a_d\}$. Note that the elements represent the action of flying forward, backward, left, right, up and down, respectively. At each time step, agent selects one action from A .

3) *Transition probability:* The transition probability function P represents the dynamic characteristic of the environment. It is intractable to model accurately due to the model-free property.

4) *Discounted factor γ :* The discounted factor γ denotes the effect of the future reward, and a larger γ indicates the decision of focusing on long-term reward.

5) *Reward function:* The reward function aims to lead the agent for achieving the goals of the task in RL process. Further, R_{t+1} is denoted as instantaneous reward of performing action a_t under current state s_t , i.e.,

$$R_{t+1}(s_t, a_t) = (-0.1 \times \Delta l)(1 - \mathcal{H}_n) + 100\mathcal{H}_n - 100\mathcal{L}_{ob}, \quad (15)$$

where Δl is the trajectory loss for each step. \mathcal{H}_n is defined as the flag for the end of the trajectory planning process, i.e.,

$$\mathcal{H}_n = \begin{cases} 0, & p_i \in \Omega, \\ 1, & p_i \notin \Omega. \end{cases} \quad (16)$$

6) *Action value function:* The action value function $Q_\pi(s, a)$ indicates the expected future reward for performing action a_t under the current state s_t , i.e.,

$$Q_\pi(s, a) = E_\pi[R_{t+1} + \gamma R_{t+2} + \gamma^2 R_{t+3} + \dots | s_t = s, a_t = a], \quad (17)$$

where a_t and s_t represent the current action and state, respectively. The cumulative discounted reward G_t is denoted as:

$$G_t = R_{t+1} + \gamma R_{t+2} + \gamma^2 R_{t+3} + \dots, \quad (18)$$

where the reward of the future time step is implied in the present step, but future rewards should be multiplied with the discounted factor γ .

C. Q-learning based QLUTP

Q-learning algorithm is a fundamental RL method. In detail, the agent chooses action $a \in A(s)$ under state s with the instruction of action value function $Q(s, a)$. Moreover, all the action value functions $Q_\pi(s, a)$ are stored in the action value table \mathcal{Q} , which is updated during the training process. Then, according to the updated \mathcal{Q} , we obtain the optimal policy π^* . The goal is to maximize the accumulated reward \mathcal{R} , i.e.,

$$\pi^* = \arg \max_{\pi} \mathcal{R}. \quad (19)$$

According to the principle of value based Q-learning algorithm, policy π^* depends on the action value table \mathcal{Q} . Thus, the policy $\pi^*(a|s)$ leads the agent to perform the action a' under state s' with the maximum $Q(s', a')$, i.e.,

$$\pi^*(a|s) = \begin{cases} 1, & a = \arg \max_{a' \in A(s')} Q(s', a'), \\ 0, & \text{otherwise,} \end{cases} \quad (20)$$

where $\max_{a' \in A(s')} Q(s', a')$ represents the max value when selecting action a' at s' .

The details of the updating process of action value table \mathcal{Q} are presented in Algorithm 2. In detail, as in step 6, it is necessary to update $Q(s_t, a_t)$ at time step t in the learning process, according to

$$Q(s_t, a_t) \leftarrow Q(s_t, a_t) + \alpha \delta_t, \quad (21)$$

where α is the learning rate, and the action value error δ_t is denoted as

$$\delta_t = R_{t+1} + \gamma \max_{a' \in A(s')} Q(s', a') - Q(s_t, a_t). \quad (22)$$

The agent performs the action a' corresponding to the optimal value $\max_{a' \in A(s')} Q(s', a')$ under the next state s' when updating $Q(s, a)$, resulting in an overestimation problem concerning the sampled action. Therefore, action selection strategy ε -greedy is introduced in traditional Q-learning method, i.e.,

$$\pi^*(a|s) = \begin{cases} 1 - \varepsilon, & a = \arg \max_{a' \in A(s')} Q(s', a'), \\ \varepsilon, & a = \text{random action,} \end{cases} \quad (23)$$

where $\varepsilon \in (0, 1)$ represents the probability of exploring random action a .

However, the traditional Q-learning method performs not well with respect to the convergence, due to the slow updating speed of \mathcal{Q} . In order to accelerate the update speed of \mathcal{Q} , an improved action selection strategy $\varepsilon(ep)$ -greedy is introduced. Further, the probability of random selection $\varepsilon(ep)$ is a function related to episodes, instead of the constant value. With the increment of episodes, the probability of selecting random action decreases, which results in faster updating of \mathcal{Q} . Thus, we design the QLUTP method to obtain an optimal trajectory ρ to minimize the total flight trajectory loss during the coverage missions.

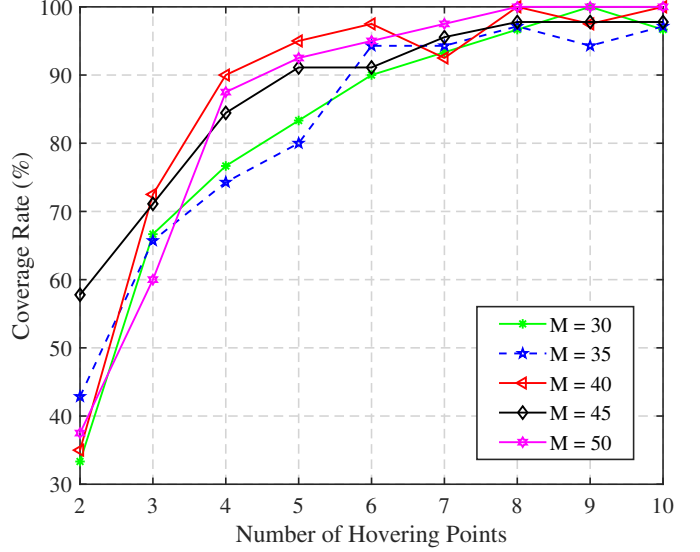


Fig. 3. Performance of coverage with different number of hovering points (Coverage rate *v.s.* Number of hovering points).

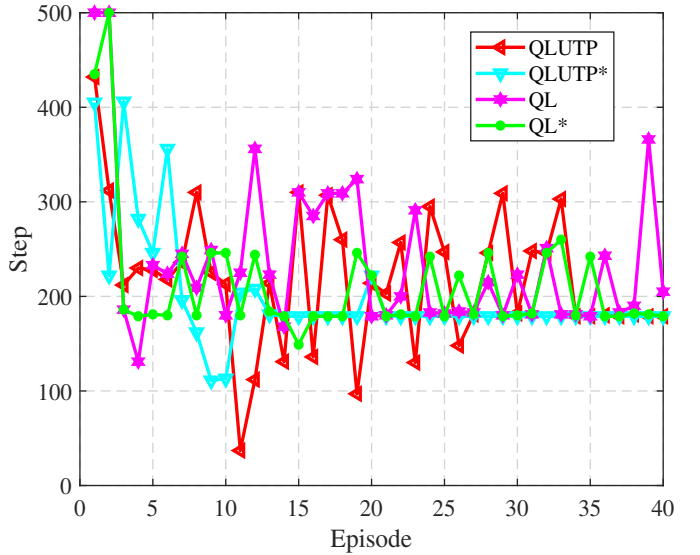


Fig. 4. Performance of convergence with different methods (Step *v.s.* Episode).

IV. SIMULATION RESULTS

The performance of the designed algorithms are evaluated in this section. Note that the locations of GUs are usually abstracted to a specific point process to capture and depict the positions in the coverage scenario. The poisson point process (PPP) is widely employed to model the distribution of GUs. Therefore, the simulations are conducted by randomly deploying the GUs following PPP. In particular, we consider a 3D coverage space ($2,000\text{m} \times 2,000\text{m} \times 200\text{m}$), and the partition accuracy is set as $\Delta l = 20\text{m}$. The flight altitude ranges from 120m to 180m. In addition, the coverage radius of the

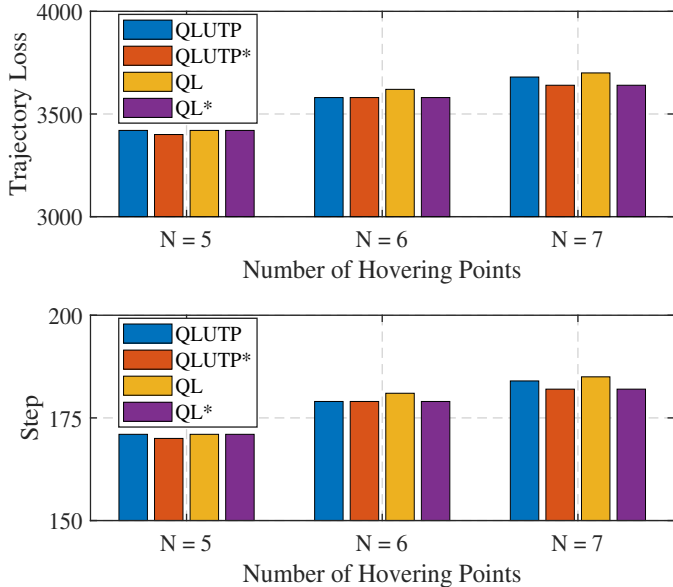


Fig. 5. Performance of trajectory planning with different methods.

UAV swarm is 500m. Further, the corresponding values of the simulation parameters about QLUTP are initially set as $(\alpha, \gamma, episode) = (0.6, 0.6, 40)$. In addition, MATLAB is used as the platform to evaluate the convergence and effectiveness of the proposed mechanisms.

As illustrated in Fig. 3, the coverage rate rises obviously with the increment of the number of hovering points N , and it gradually converges and oscillates within a certain range slightly. The coverage rates under several scenarios with different number of GUs, i.e., $(M = [30, 35, 40, 45, 50])$, show that the average coverage rate is evidently above 90% when $N = 6$. Finally, the optimal hovering points $\Omega(q_1 \rightarrow q_6, \mathcal{Y})$ is obtained.

To evaluate the performance of the proposed trajectory planning method, Fig. 4 indicates the convergences of the proposed QLUTP and QLUTP* obtained by different action selection strategies $\varepsilon^*(ep)$, compared with other methods. Note that the fastest convergence of QLUTP* reveals the superiority and effectiveness of Algorithm 2. Moreover, the trajectory loss of different algorithms for three scenarios are shown in Fig. 5. Specifically, we select four methods for trajectory planning under different HPs sets. It is shown that the distance of trajectory increases significantly with N increasing, which indicates that the UAV swarm consumes more flight energy. In addition, the optimal trajectory planned by QLUTP* needs fewer steps with less trajectory loss.

V. CONCLUSIONS

In this work, we propose a hierarchical framework for the UAV swarm to handle the ACP for large-scale 3D coverage scenario. The UAV swarm provides steady wireless communication for non-uniformly distributed GUs. Additionally, K-means

method is adopted to cluster GUs and select appropriate HPs. Further, according to the MDP model, we propose a QLUTP approach for trajectory planning. Simulations are conducted to evaluate the performance of the proposed method, and the results demonstrate that the proposed algorithms perform better for ACP than other baseline methods.

REFERENCES

- [1] Z. Jia, M. Sheng, J. Li, D. Niyato, and Z. Han, "LEO-Satellite-Assisted UAV: Joint trajectory and data collection for Internet of remote things in 6G aerial access networks," *IEEE Internet Things J.*, vol. 8, no. 12, pp. 9814–9826, Jun. 2021.
- [2] A. R. Yusoff, N. Darwin, Z. Majid, A. F. Razali, and M. F. M. Ariff, "Beach volume measurement on variation of UAV altitude mapping," in *2020 IEEE 10th International Conference on System Engineering and Technology (ICSET)*, Shah Alam, Malaysia, 2020.
- [3] X. Liu and N. Ansari, "Resource allocation in UAV-Assisted M2M communications for disaster rescue," *IEEE Wireless Commun. Lett.*, vol. 8, no. 2, pp. 580–583, Nov. 2019.
- [4] Y. Zhang, Z. Mou, F. Gao, J. Jiang, R. Ding, and Z. Han, "UAV-Enabled secure communications by multi-agent deep reinforcement learning," *IEEE Trans. Veh. Technol.*, vol. 69, no. 10, pp. 11 599–11 611, Oct. 2020.
- [5] J. You, Z. Jia, C. Dong, L. He, Y. Cao, and Q. Wu, "Computation offloading for uncertain marine tasks by cooperation of UAVs and vessels," in *ICC 2023 - IEEE International Conference on Communications*, Rome, Italy, 2023.
- [6] C. Cui, Z. Jia, C. Dong, Z. Ling, J. You, and Q. Wu, "Distributionally robust chance-constrained optimization for hierarchical UAV-based MEC," in *INFOCOM 2023 DroneCom: 6th International Workshop on Drone-Assisted Wireless Communications for 5G and Beyond*, New York, USA, 2023.
- [7] Y. Nie, J. Zhao, J. Liu, J. Jiang, and R. Ding, "Energy-efficient UAV trajectory design for backscatter communication: A deep reinforcement learning approach," *China Commun.*, vol. 17, no. 10, pp. 129–141, Oct. 2020.
- [8] Y. Zeng and R. Zhang, "Energy-efficient UAV communication with trajectory optimization," *IEEE Trans. Wireless Commun.*, vol. 16, no. 6, pp. 3747–3760, Jun. 2017.
- [9] X. He, W. Yu, H. Xu, J. Lin, X. Yang, C. Lu, and X. Fu, "Towards 3D deployment of UAV base stations in uneven terrain," in *2018 27th International Conference on Computer Communication and Networks (ICCCN)*, Hangzhou, China, 2018.
- [10] Z. Jia, Q. Wu, C. Dong, C. Yuen, and Z. Han, "Hierarchical aerial computing for Internet of things via cooperation of HAPs and UAVs," *IEEE Internet Things J.*, vol. 10, no. 7, pp. 5676–5688, Apr. 2023.
- [11] Q. Hou, Y. Cai, Q. Hu, M. Lee, and G. Yu, "Joint resource allocation and trajectory design for Multi-UAV systems with moving users: Pointer network and unfolding," *IEEE Trans. Wireless Commun.*, vol. 22, no. 5, pp. 3310–3323, May 2023.
- [12] X. Chen, J. Tang, and S. Lao, "Review of Unmanned Aerial Vehicle swarm communication architectures and routing protocols," *Appl. Sci.*, vol. 10, no. 10, p. 3661, May 2020.
- [13] P. S. Agram and H. A. Zebker, "Sparse Two-Dimensional phase unwrapping using regular-grid methods," *IEEE Geoscience and Remote Sensing Letters*, vol. 6, no. 2, pp. 327–331, Apr. 2009.
- [14] Z. Ma, B. Ai, R. He, G. Wang, Y. Niu, and Z. Zhong, "A wideband non-stationary Air-to-Air channel model for UAV communications," *IEEE Trans. Veh. Technol.*, vol. 69, no. 2, pp. 1214–1226, Feb. 2020.
- [15] Z. Mou, Y. Zhang, F. Gao, H. Wang, T. Zhang, and Z. Han, "Deep reinforcement learning based Three-Dimensional area coverage with UAV swarm," *IEEE J. Sel. Areas Commun.*, vol. 39, no. 10, pp. 3160–3176, Oct. 2021.
- [16] A. Al-Hourani, S. Kandeepan, and S. Lardner, "Optimal LAP altitude for maximum coverage," *IEEE Wireless Commun. Lett.*, vol. 3, no. 6, pp. 569–572, Dec. 2014.